Evaluation of unsaturated zone water fluxes in heterogeneous alluvium at a Mojave Basin Site

John R. Nimmo and Jeffrey A. Deason[1]
U.S. Geological Survey, Menlo Park, California, USA

John A. Izbicki and Peter Martin
U.S. Geological Survey, San Diego, California, USA

Received 19 June 2001; revised 12 November 2001; accepted 15 April 2002; published 29 October 2002.

[1] Vertical and horizontal water fluxes in the unsaturated zone near intermittent streams critically affect ecosystems, water supply, and contaminant transport in arid and semiarid regions. The subsurface near the Oro Grande Wash is typical in having great textural diversity, pronounced layer contrasts, and extremely low hydraulic conductivities associated with nearly dry media. These features prevent a straightforward application of the Darcian method for recharge estimation, which has provided high-quality flux estimates at simpler, wetter sites. We have augmented the basic Darcian method with theoretical developments such that a small number of core sample unsaturated hydraulic property measurements, combined with additional, easily obtained data (e.g., drillers' logs) can provide useful flux estimates and knowledge of two-dimensional water behavior beneath the wash. *INDEX TERMS:* 1824 Hydrology: Geomorphology (1625); 1829 Hydrology: Groundwater hydrology; 1866 Hydrology: Soil moisture; 1875 Hydrology: Unsaturated zone; 1884 Hydrology: Water supply; *KEYWORDS:* unsaturated zone, vadose zone, recharge, flux measurement, stratification, Darcian flow

Citation: Nimmo, J. R., J. A. Deason, J. A. Izbicki, and P. Martin, Evaluation of unsaturated zone water fluxes in heterogeneous alluvium at a Mojave Basin Site, *Water Resour. Res.*, *38*(10), 1215, doi:10.1029/2001WR000735, 2002.

1. Introduction

[2] The low precipitation and high evapotranspiration rates in arid regions can cause the deep unsaturated zone, defined as the portion of the unsaturated zone below the deepest plant roots, to have considerable thickness. Vertical and horizontal water fluxes in this zone are a dominant influence on aquifer recharge, solute travel times, and other hydrologic processes. Water flowing downward in this zone is generally called deep drainage or deep percolation, some of which may enter the aquifer as recharge. A measurement of deep drainage in the case where essentially all of it reaches the water table thus may serve as an aquifer recharge measurement. Especially where recharge is associated with particular topographic or geologic features (e.g. stream channels), horizontal fluxes in the unsaturated zone may disperse the vertical flow, thereby reducing recharging flux densities and complicating this determination.

[3] The deep unsaturated zone in arid regions typically is low in water content, so that unsaturated hydraulic conductivity is small and liquid fluxes are small or negligible. Exceptions may occur beneath stream channels and lake beds where surface water collects. These features may contribute significant aquifer recharge even in desert lands where vertical fluxes may be negligible over large expanses between such topographically low features. The Oro Grande Wash in the Mojave River Basin near Victorville, California (Figure 1) is one such area where intermittent streamflow may be a significant source of aquifer recharge through a thick (up to 300-m) unsaturated zone [*Izbicki et al.*, 2000b]. An additional complicating feature of this and many other field sites is the hydraulic effect of sharply contrasting layers in the unsaturated zone [*Li et al.*, 2001].

[4] Many past approaches to the estimation of fluxes in the deep unsaturated zone, summarized for example by *Simmers* [1988], address the problem in terms of total recharge at the scale of watersheds and basins. Methods that produce point estimates of recharge rates are also valuable, to permit smaller scale studies as well as to investigate variability, anisotropy, lateral flow, and other local and process-related hydrologic influences. With a large number of point measurements of water flux, or with a modest number of measurements supplemented by information on landscape features, it would be possible to infer areal recharge rates [*Nimmo et al.*, 2000].

[5] One approach with potential for accurately estimating point recharge rates is to determine the flux density (q, the vertical component of which is the rate of deep drainage) from measurements of unsaturated hydraulic conductivity (K) and matric pressure (ψ) gradients in the deep unsaturated zone, assuming water is driven downward according to Darcy's law [*Nimmo et al.*, 1994]. In cases where the ψ gradient is negligible, the only difficult measurement is that of K at the water content that exists at the point of q determination.

[1]Now at LECG, LLC, Palo Alto, California, USA.

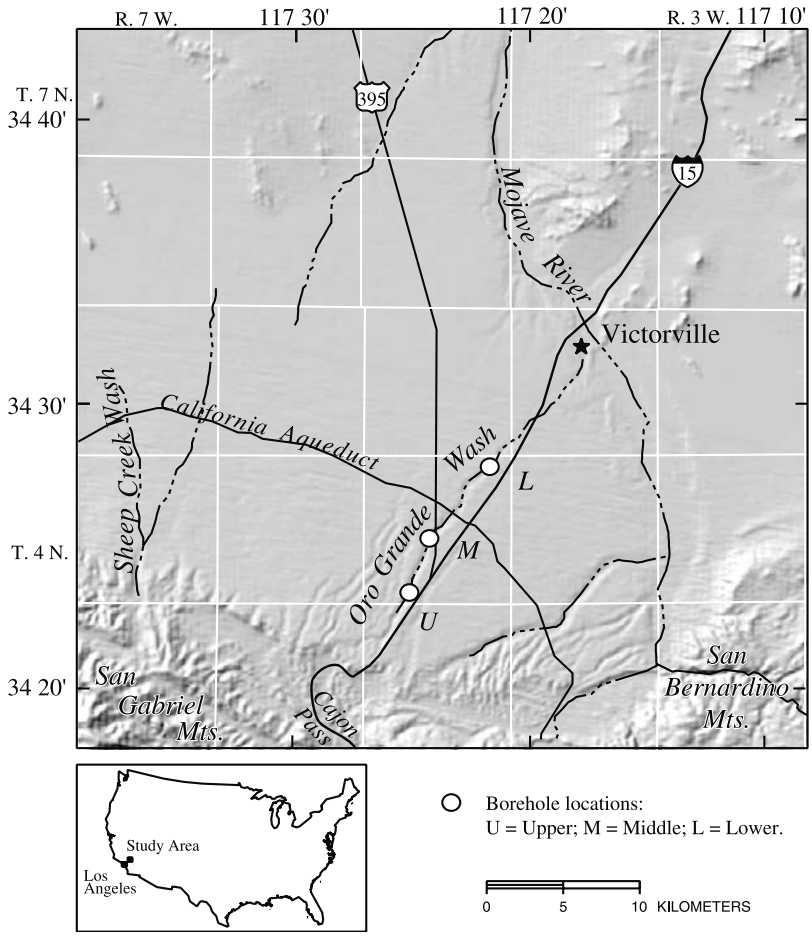

Figure 1. The study area, with upper, middle, and lower borehole sites marked along the Oro Grande Wash, and hydrogeologic features as described by *Mendez and Christensen* [1997] and *Izbicki et al.* [2000a].

[6] *Nimmo et al.* [1994] used this method for point recharge estimates in the Palouse region of Southeastern Washington, where the unsaturated zone comprises deep loess deposits that are unusually uniform in texture and structure, and are essentially devoid of coarse particles. Also, the 50 cm/yr of precipitation at this site makes it likely that there is significant recharge from areally diffuse infiltration even in the absence of stream-channel focusing. As water goes deeper within the deep unsaturated zone of a relatively simple medium such as the Palouse loess deposits, the flow rates go through a process of physical averaging and homogenizing. At depths deep enough that this process is essentially complete, even a single point measurement may indicate the long- term average recharging flux over an area of uniform hydrologic characteristics.

[7] Our main objective in this study is to estimate prevailing unsaturated-zone vertical and horizontal water fluxes near the Oro Grande Wash of the Mojave River Basin, and interpret them in ways relevant to estimation of recharge rates and contaminant travel times. The steps are (1) to obtain unsaturated-zone core samples from depths of at least several meters, (2) to measure core-sample properties, especially hydraulic conductivity as a function of water content over a range that includes or comes as close as possible to the field water content, and (3) to infer water fluxes by interpretation of simulations based on the measured properties and supplemental information from field observations.

[8] Compared to the Palouse region, the Mojave River Basin has features more typical of arid-region unsaturated zones: alluvial deposits with layers of sharply contrasting texture, considerable gravel in most layers, and precipitation so low that recharge is probably significant only where surface features concentrate runoff. The presence of texturally contrasting layers and other inhomogeneities complicates the verification of the steadiness of flow and the determination of the true driving force. Given these complexities, one cannot assume that the deep unsaturated zone is uniform enough to satisfy the simplifying condition of negligible matric pressure gradients. The flow, even if steady, may be driven by these gradients in addition to gravity. Thus it is necessary to determine the actual net driving force at the locations of samples, or at least to quantify the uncertainty arising from imperfect knowledge of this net force. An additional challenge is that one cannot depend on physical averaging to be done by the unsaturated porous medium itself. Hypothetically, a brute-force characterization of flow would be possible by measuring the flux at a large number of points and averaging them with an appropriate algorithm. In practice the large number of measurements needed for this is impossible because of limitations of resources and of the medium itself. In this

paper we demonstrate a means of combining a few accurate measurements of unsaturated hydraulic conductivity relations with a large amount of easily obtained information (e.g., basic textural descriptions of the subsurface media) to assess water fluxes relevant to aquifer recharge.

2. Oro Grande Wash Site

[9] The study area is the upper part of the Mojave River Basin, in the western part of the Mojave Desert about 130 km east of Los Angeles, California (Figure 1). The climate has low humidity and high summer temperatures. Precipitation in most of the area is generally less than 15 cm/yr, though precipitation in the San Bernardino and San Gabriel Mountains to the south can exceed 100 cm/yr, much of it falling as snow.

[10] The Oro Grande Wash is deeply incised (about 10 to 20 m) into the surface of the regional alluvial fan and streamflow along the wash has followed nearly the same course for about 500,000 years [*Meisling and Weldon*, 1989]. Because the head of the fan has been eroded by Cajon Creek (which drains to the Pacific Ocean), the Oro Grande Wash no longer drains the San Bernardino or San Gabriel Mountains. Streamflow in the wash is a combination of runoff from precipitation near Cajon Pass and locally derived runoff on the desert floor. Runoff from large storms that typically occur a few times each year allows intermittent streamflow in the wash. The width of the wetted channel when it flows is typically about 2 to 5 m. On the basis of channel geometry data developed by *Lines* [1995], average annual flow in Oro Grande Wash was estimated to be about 6×10^5 m^3/yr in the middle of the wash, near Highway 395, and 4×10^4 m^3/yr about 15 km downstream, at the Mojave River.

[11] The study area has an alluvial aquifer that is extensively pumped. In some places water levels have dropped more than 0.3 m/yr over the last several years [*Mendez and Christensen*, 1997]. The unsaturated zone overlying this aquifer ranges from about 300 m near the mountain fronts to more than 60 m thick towards the basin [*Stamos and Predmore*, 1995].

[12] The subsurface media in the study area are mostly sandy alluvial materials, with substantial amounts of gravel, in distinct depositional layers. The particle-size distribution and general character of these materials vary widely from place to place, from layer to layer, and within layers.

3. Methods

[13] Gravitational and matric pressure gradients drive water downward through the unsaturated zone, as expressed by Darcy's law:

$$q = -K(\Psi)\left[\frac{d\Psi}{dz} + pg\right] \quad (1)$$

where q is the flux density (flux per unit area, equivalent to Darcy velocity), ψ is the matric pressure, K is the hydraulic conductivity (considered as a function of ψ, z is the vertical coordinate, ρ is the density of water, and g is the gravitational acceleration. Figure 2 illustrates ψ profiles that can develop in a thick unsaturated zone. Near the surface, changes in moisture with time cause matric pressure to fluctuate with depth. If the unsaturated zone is sufficiently deep, these fluctuations become completely damped, creating a zone of constant flux [*Gardner*, 1964]. In this zone, if the medium is homogeneous, matric pressure is uniform with depth and gravity is the only force driving downward flow.

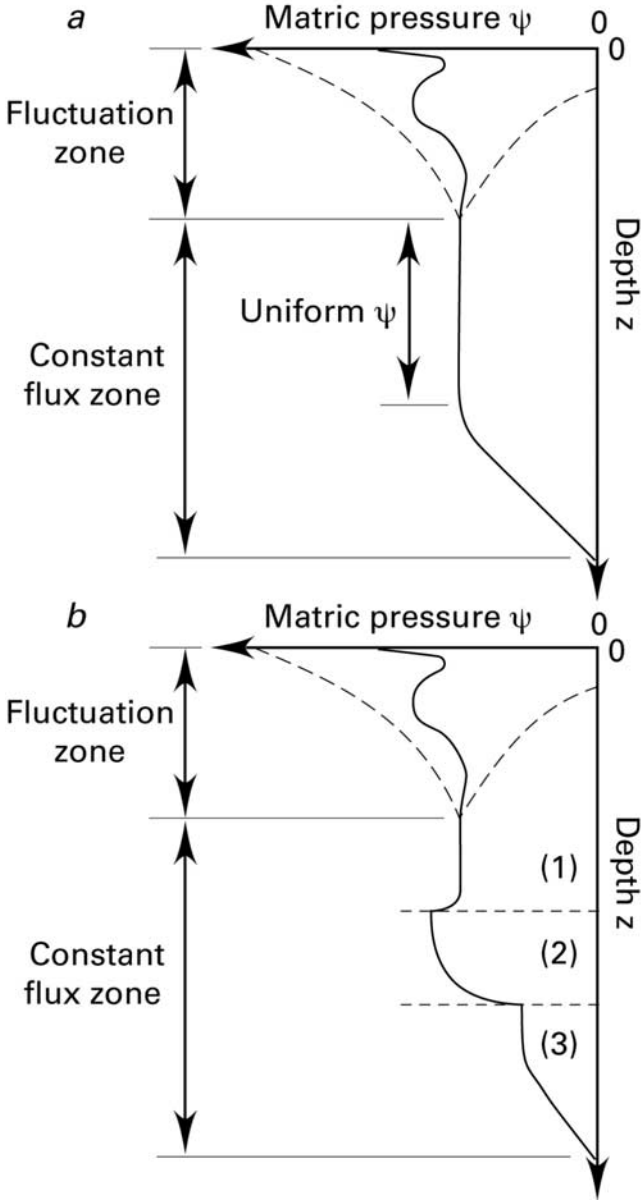

Figure 2. Hypothetical profiles of matric pressure as a function of depth in an unsaturated zone deep enough that its lower portion has a constant downward flux of water in (a) a uniform and (b) a layered profile. Dashed curves indicate possible extremes in the upper portion. The lowest horizontal line in each diagram indicates the position of the water table.

[14] Measurements on core samples can yield values for K at various water contents. If the sample comes from a zone where the flow is steady and driven by gravity alone, the measured K at the existing water content indicates the downward flux density, q, which is interpretable as a long-term average recharge rate as described above. Such a determination is possible by applying the steady state centrifuge (SSC) method for K measurement [*Nimmo et al.*, 1987].

Because this approach requires an unsaturated zone of at least moderate depth and because the SSC method works well for small K values, it is particularly attractive for use in arid regions.

[15] In a layered medium (Figure 2b), the constant-flux portion of a deep unsaturated zone would be uniform in q, but not in ψ or water content (θ). If layers are sufficiently thick, a uniform ψ zone can develop within each [*Childs*, 1969]. K measurement for a sample from the uniform-ψ zone in any layer would still indicate q, though the uniformity of ψ is in doubt if the sample is from the vicinity of a layer transition.

3.1. Sampling

[16] Three unsaturated-zone monitoring sites were used as part of this study and designated upper, middle, and lower (U, M, L), according to elevation. Holes at these sites were drilled using the underreamer air hammer method [*Driscoll*, 1986; *Hammermeister et al.*, 1986]. This drilling method uses steel casing (in this case 20 cm in diameter) to stabilize the borehole during drilling. Drill cuttings are discharged through the casing and undisturbed soil core can be collected through the bottom of the casing during the drilling process. Because the well casing follows the underreamer drill bit, drilling fluids are not required to stabilize the borehole. Drill depths ranged from 30 m to 170 m. The diameter of the boreholes was 20 cm. The underreamer drilling method minimized disturbance of the unsaturated material near the borehole, minimized contamination from drilling fluids, and allowed the collection of high-quality cuttings and cores. Because the core sampler moves into new material ahead of the cutting bit, exposure of the core samples to air is minimal; given the volume of material in these samples, evaporative changes in their net water content during sampling should be negligible. Between drilling operations the casing was sealed to prevent air movement into and out of the hole. Figure 1 shows the locations of boreholes used in this study.

[17] At depths less than 30 m, cuttings were collected every 30 cm, and 60-cm cores were collected within every 1.5-m interval using a 9-cm or a 10-cm diameter piston core barrel. Deeper than 30 m, both cuttings and cores were collected less frequently. Drilling rates were coordinated with sample collection to allow cuttings from discrete intervals to be collected. The core barrel was lined with 15-cm-long brass or aluminum core liners. Cores and core liners extruded from the core barrel were capped with plastic caps and sealed with electrical tape, then wrapped in plastic and saved in a heat-sealed aluminum pouch. *Izbicki et al.* [2000a] give additional details of field sampling and site instrumentation.

[18] Detailed lithologic logs were compiled from descriptions of drill cuttings and core material collected at each borehole. In the field, cuttings and core material were described by texture, sorting, rounding, color, mineralogy, and any other significant observable feature. In the laboratory, cuttings and core material were reexamined and described in greater detail. The core samples were unwrapped and recored into 5-cm diameter, 4-cm high retainers using a motorized extrusion device [*Nimmo and Mello*, 1991]. Some surfaces of the core sample were briefly exposed to laboratory air during this process, though the material most affected in this way was trimmed away and discarded. The initial water contents of the core samples that were measured using the SSC method were obtained from the initial weight of each sample after recoring. This calculation used all pertinent tare weights of apparatus and the final oven-dry soil mass. As with the measurements of *Nimmo et al.* [1994], it was important to do the water content determination for exactly the material used in the SSC measurements, excluding any water content information from discarded portions of the original sample, because the flux determinations inferred from the $K(\theta)$ data are very sensitive to the value of the field water content. For some core samples, matric pressure measurements were made in a laboratory of the Desert Research Institute shortly after core retrieval [*Izbicki et al.*, 2000a]. Three techniques were applied for these matric pressure measurements: tensiometers for the wettest samples, the filter- paper method [*Campbell and Gee*, 1986] for other samples with $\psi > -10^4$ cm-water, and the chilled-mirror hygrometer method [*Gee et al.*, 1992] for samples with $\psi < -10^4$ cm-water.

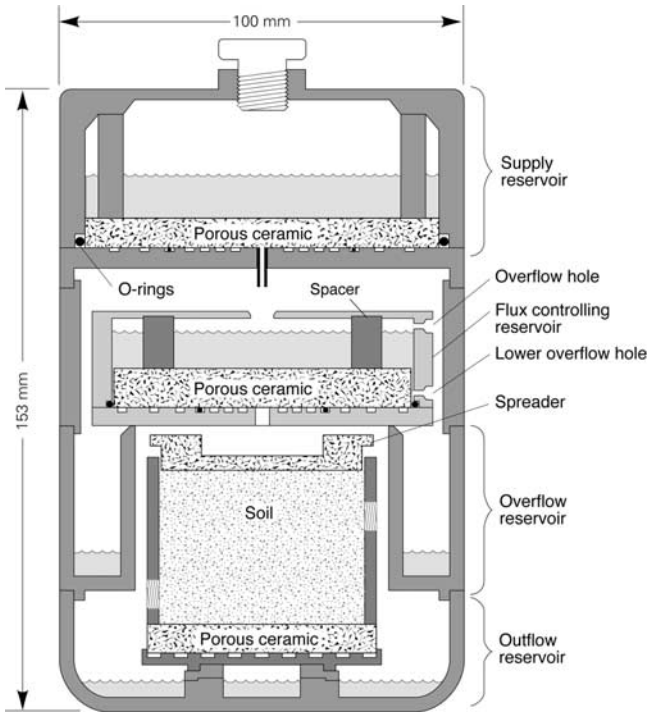

Figure 3. Apparatus fitting into a 1-L centrifuge bucket for establishing and measuring steady state flow through the sample [*Nimmo et al.*, 1992, 1994], in which one reservoir controls flux and a separate applicator spreads water over the sample.

3.2. Measurement of Hydraulic and Bulk Properties

[19] The SSC method establishes steady flow in a sample with a known body force in a way that permits measurement of the flux density. The centrifugal force allows accurate measurements at the low K values applicable in this study. Evidence of *Nimmo and Akstin* [1988] suggests that for sandy materials under conditions of interest here, the effects of centrifugal compaction on the measured hydraulic properties will be negligible.

[20] The SSC apparatus used in this study (Figure 3) is essentially that of *Nimmo et al.* [1994], including the

adaptation by *Nimmo et al.* [1992]. It includes a constant-head reservoir with an overflow hole that maintains a constant level of water above a ceramic plate (B) in a centrifugal field. A second ceramic plate spreads the water to infiltrate into the sample. When this apparatus establishes steady flow, q is known from measured changes in weight of the various reservoirs that spin with the sample in the centrifuge bucket. Then if the ψ gradient along the sample length is known or known to be negligible, Darcy's law gives K from the formula

$$q = -K\left[\frac{d\Psi}{dr} - \rho\omega^2 r\right] \tag{2}$$

where r is the distance from the center of rotation, ρ is the density of water, and is the centrifuge angular speed. The sample weight measured after centrifugation provides data for eventual calculation of the average θ to be associated with the measured K. Similarly, a tensiometer brought into contact with the sample gives the corresponding ψ value. Repeating the measurements with appropriate choices of q and gives a set of (K, θ, ψ) data characterizing the sample [*Nimmo et al.*, 1987]. The ψ and θ values also are used as data points to determine the water retention curve, $\psi(\theta)$.

[21] After the unsaturated measurements, we measured the saturated hydraulic conductivity by the gravity-driven falling-head method [*Klute and Dirksen*, 1986]. In this measurement the water was initially ponded about 10 cm above the sample in a 6-cm-diameter acrylic tube. A depth micrometer indicated the declining level of the water over time.

[22] After all of the hydraulic measurements, we oven-dried the samples and computed their bulk densities. The volume used in the bulk density calculation was computed from the dimensions of the cylindrical sample retainer and was corrected for any recesses present on either face of the sample. We computed the porosities using the average measured particle density of 2.7 g/cm^3.

[23] We measured the particle size distribution of samples from selected depths, including those for which hydraulic properties were measured. For this we used a Coulter LS100 optical particle size analyzer (mention of product names does not constitute endorsement by the U.S. Geological Survey), supplemented by sieving for particles larger than 800 microns. Each optical measurement required approximately 0.3 g of material. Samples larger than this were split using a spinning riffler. Pretreatment of the sample included 10 minutes in an ultrasonic bath to disperse the soil.

3.3. Numerical Simulations

[24] We used two numerical simulators for water flow in the unsaturated-zone profile beneath the wash to help explain the variation in vertical flux implied by the *K* measurements, as explained by *Deason* [1997]. The first, a one-dimensional model, solves Darcy's law using an adaptive-stepsize Runge-Kutta method [*Press et al.*, 1989]. *Nimmo et al.* [1987, 1994] used a similar Runge-Kutta model to solve Darcy's law in related applications. To represent the $K(\psi)$ function we used the empirical formula of *Gardner* [1958]:

$$K(\Psi) = \frac{K_{sat}}{1 + \left(\frac{\Psi}{\Psi_o}\right)^n} \tag{3}$$

where ψ_o and n are fitted parameters and K_{sat} is the saturated K. Given q and $K(\psi)$ specified as values of the three parameters K_{sat}, ψ_o, and n, the model solves (1) for $\psi(z)$.

[25] The second simulator is a two-dimensional model constructed using the U.S. Geological Survey code VS2DT [*Lappala et al.*, 1987; *Healy*, 1990]. This code solves Richards' equation

$$\left(\frac{d\theta}{d\Psi}\right)\frac{\partial\Psi}{\partial t} = \nabla \bullet (K\nabla\Psi) + pg\frac{\partial K}{\partial z} \tag{4}$$

in two dimensions using a finite differencing method to find matric pressures and other conditions at various positions. The domain of simulation covered 40 m laterally from the center of the stream channel, and 185 m vertically. Laterally the grid had 20 nodes, with unequal spacing increasing with distance from the stream. Vertically the grid had 335 nodes, with equal 0.1-m spacing for the uppermost 30 m, and greater spacing below. The upper boundary condition was a constant, nonzero flux over 0.5 m laterally to represent the half-width of the stream channel, and zero flux elsewhere. The lower boundary condition was zero matric pressure representing the water table. Other boundary points were simulated with a zero flux condition. The effects of boundaries on the essential results were minimized by the domain of interest being much smaller than the domain simulated, including about 5 of the 40 m laterally and 30 of the 185 m vertically. We forced the program to simulate a steady state condition by setting the residual water content parameter equal to the porosity. The moisture retention curve used by VS2DT is then flat, causing $d\theta/d\psi$ to be zero and removing the time-dependent term in Richards' equation (4). This adaptation causes this code to produce iteratively closer approximations to the steady-state solution while retaining the appropriate unsaturated values of $K(\psi)$ and $\theta(\psi)$ in calculating the finite-difference solution (R.W. Healy, private communication, 1996). In these calculations we also set the specific storage term to a negligibly small value, though still finite and positive to avoid numerical difficulties.

4. Results

4.1. Samples

[26] For successful extrusion and recoring, samples had to be almost completely free of gravel or larger particles, and had to be cohesive enough to retain structural integrity. Only about one Oro Grande Wash sample in 10 came from a layer sufficiently free of large particles and wet enough for adequate cohesion. Core samples from the alluvial fan outside of the Oro Grande Wash and from beneath another nearby ephemeral stream channel were too dry, and crumbled with any attempt to put them into the SSC apparatus. Five samples were usable, two each from the lower and middle, and one from the upper Oro Grande Wash holes. These had mostly very fine to medium sand, with some silty material and very little to no gravel. To mitigate the effects of bias due to the nonrepresentative nature of this set of samples, we made various accommodations in flow modeling efforts and interpretation of the results, described below. In this paper we identify individual samples by the

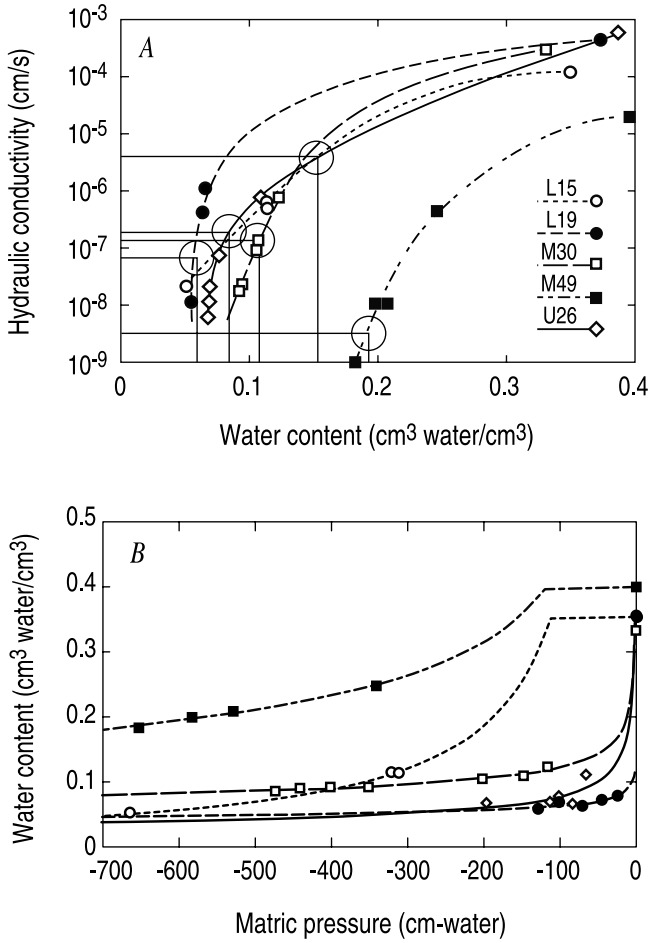

Figure 4. Steady state centrifuge measurements of (a) hydraulic conductivity and (b) water retention, for five samples from the Oro Grande Wash. Measurements as point symbols are shown with fitted curves. The wettest point in each case is from ordinary gravity-driven steady state or falling head methods for K_{sat}. Field water contents and their corresponding hydraulic conductivities (for q estimates) are indicated on Figure 4a.

Oro Grande Wash hole they came from (U, M, or L) and the sample depth in meters (for example, M30).

4.2. Measurements

[27] Figure 4 shows hydraulic property results for the five Oro Grande Wash core samples. The properties are typical of materials with these textures. Measurement uncertainty in K is about ±20%, computed by combining measurement errors estimated for each type of primary data (readings of balances, timers, etc.). Because of soil-water hysteresis and changes in sample properties over the duration of the measurements, this is greater than the ±7% uncertainty sometimes achievable with the SSC method [*Nimmo et al.*, 1987]. Figure 4a also indicates the estimated downward flux densities determined by selecting the value of K corresponding to the field water content of each core, under the assumption that flow is entirely gravity-driven. Figure 5 shows these q values as a function of depth for the three holes.

[28] For three cores at intermediate depths, the estimated q varies modestly, between 2 and 6 cm/yr. For the other two cores, however, q is very different: 0.1 and 130 cm/yr. If the actual flow is steady and downward at these depths, q in each hole would have to be independent of depth. Thus the two divergent values indicate a violation of one or more assumptions associated with these estimates.

[29] Two of the working assumptions to reconsider are that the flow is steady and that the matric-pressure gradients are negligible. Steadiness cannot be established directly from our one-time sampling, but can be evaluated with respect to self-consistency of the larger hydrologic picture inferred from the data. The matric pressure in a layered medium will not be uniform, even with steady flow (Figure 2b). A nonuniform matric pressure, with steady or unsteady flow, violates the assumption of unit gradient. If ψ gradients are great enough to invalidate the assumption of gravity-driven flow, as might result from substantial variations in hydraulic properties associated with textural contrasts between layers, the water fluxes will be incorrectly inferred. Any of the five flux estimates could be erroneous because of this problem. We undertook the modeling study to test the likelihood that nonuniformities of matric pressure associated with pronounced layering may cause significant

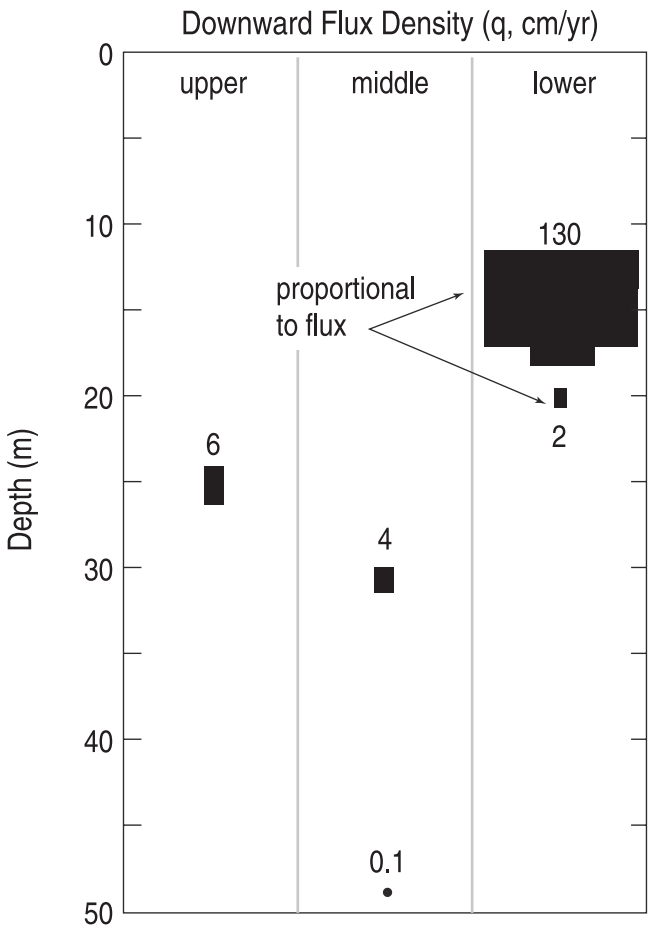

Figure 5. Hypothetical downward flux densities, computed from the K(θ) data in Figure 4a, with the assumption that the flow is driven solely by gravity, as a function of depth for three boreholes (upper, middle, and lower as designated in Figure 1) in the Oro Grande Wash. Areas of symbols are proportional to the flux density.

Table 1. Fitted and Scaled Parameters for Equation (3) k Relations[a]

Parameter	L15	M30	L19	U26	Gravel [*Fayer et al.*, 1992]	Average
λT, cm	0.0090	0.03	0.062	0.07	1.0	
K_{sat}, cm/s	9.4×10^{-5}	2.7×10^{-4}	3.5×10^{-4}	5.5×10^{-4}	3.5×10^{-1}	
λo, cm-water	−94	−10	−21	−6.4	−.21	−26
N	4.5	2.6	5.1	3.5	6.05	4.4
K_{sat}/λ^2	1.2	.3	.09	0.11	0.35	0.41
$\Psi o\ \lambda$	−0.846	−.3	−1.3	−0.45	−0.21	−0.62

[a] The scaling parameter λ is taken here as the mean particle size.

errors in the fluxes inferred from K measurements. An additional purpose was to help assess the effect of layering on lateral flow away from the wash. This is critical for estimating the total recharge from a given segment of channel reach.

4.3. Hydraulic Property Estimates for All Layers

[30] The models require information about hydraulic properties of the media, specifically, a $K(\psi)$ function, as input. To model the continuous, multilayered unsaturated-zone profile, we generated surrogate hydraulic property data to supplement the high-quality measurements on the one or two samples per borehole. For this purpose, we applied scaling techniques to estimate values of the parameters ψ_o, K_{sat}, and n of the empirical $K(\psi)$ formula (3), for each layer known from the lithology logs. We assumed that the media in all layers are Miller similar, that is that the properties of any layer are equivalent to those that would be obtained from a medium that is a scale magnification of another layer [*Miller and Miller*, 1956; *Miller*, 1980]. The hydraulic properties scale with a geometric factor λ, which we took for convenience to equal the mean grain size. By Miller similitude and capillary theory, ψ_0 varies inversely with λ because an interfacial pressure within a capillary is inversely proportional to the radius of curvature and hence to the capillary radius. K_{sat} varies directly with the square of λ analogously to Poiseuille's law. By Miller similitude, the parameter n has no relationship to λ and is therefore a constant.

[31] With the similarity assumption, properties of unmeasured layers could be scaled from those of a base set of parameter values derived from those of the measured samples (Table 1). To counter the bias of our measured data set toward fine-textured samples, we included data from *Fayer et al.* [1992] for a coarse gravel. Although this material came from a different site, hydraulic properties of such a coarse material are likely to be dominated by texture more than structural arrangement or mineralogy, in which case it would approximate the properties of a similarly gravelly layer of the Oro Grande Wash site. The first step in generating the base parameter values was to compute optimized parameter values for each sample. We did this by fitting equation (3) to the measured $K(\psi)$ data by linear regression on the logarithms of the data. This is a suitable procedure because when log-transformed, (3) is a linear equation. We then divided these estimated parameter values by their theoretical scaling relationship with their sample's mean grain size λ, as shown in Table 1. Data for sample M49 are omitted because they were unavailable for the initial scaling computations. This omission has minor quantitative influence on the succeeding predictions of ψ profiles, but as shown below in sensitivity calculations, does not affect the water flux determinations that are the chief objective of the study. For each of the three parameters ψ_o, K_{sat}, and n, we averaged the results among the samples to reach a base value to be scaled.

[32] For each layer without core-sample measurements, to determine ψ_o and K_{sat} parameter values we applied the appropriate Miller-Miller scaling relationship to the base values and the estimated mean grain size of the layer. The fact that the n values in Table 1 vary little (about a factor of two, for the factor-of-100 variation in λ) support the Miller-similitude assumption of no scale dependence of n. Thus the base value of n could be used directly for any layer.

[33] For most layers, grain size measurements were unavailable, so we estimated the mean grain size values through a systematization of layer descriptions in lithology logs that had been compiled during drilling (see Appendix A). Once the mean grain sizes were calculated and the $K(\psi)$ functions established for each layer, the model could generate a complete vertical profile of ψ for a given hole, at any given steady q.

4.4. One-Dimensional Numerical Simulations

[34] Our one-dimensional model of downward flow through the layered unsaturated zone estimates the effect of different layers and layer boundaries on matric pressure gradients and tests the error resulting from the assumption that these gradients are negligible.

[35] Two sets of simulation results from the lower hole, with flux densities of 3 cm/yr and 0.03 cm/yr, are shown in Figure 6; other results from this and other holes have the same general character in terms of profile shape elements and the way they join together. Each profile has numerous short intervals that are nearly straight and vertical; between these are intervals that show steeper gradients. A given sample may have come from a 4-cm segment of the profile that either does or does not include an interval with a steep gradient. Because the precise vertical position of any given feature is known only to the nearest 30 cm, the precision of layer thicknesses and positions in the lithology logs, it is not possible to use the profiles in Figure 6 to ascertain whether a specific sample is from an interval with an acceptably small gradient. The modeled profiles, however, can be assumed to represent significant features of the actual profiles, though not at the exact depth. This makes them useful for evaluating the probability that the ψ gradient in any given core-sized interval is small enough that the vertical flux inferred for that core can be accepted with reasonable confidence. To quantify the acceptability of results for a core sample, we

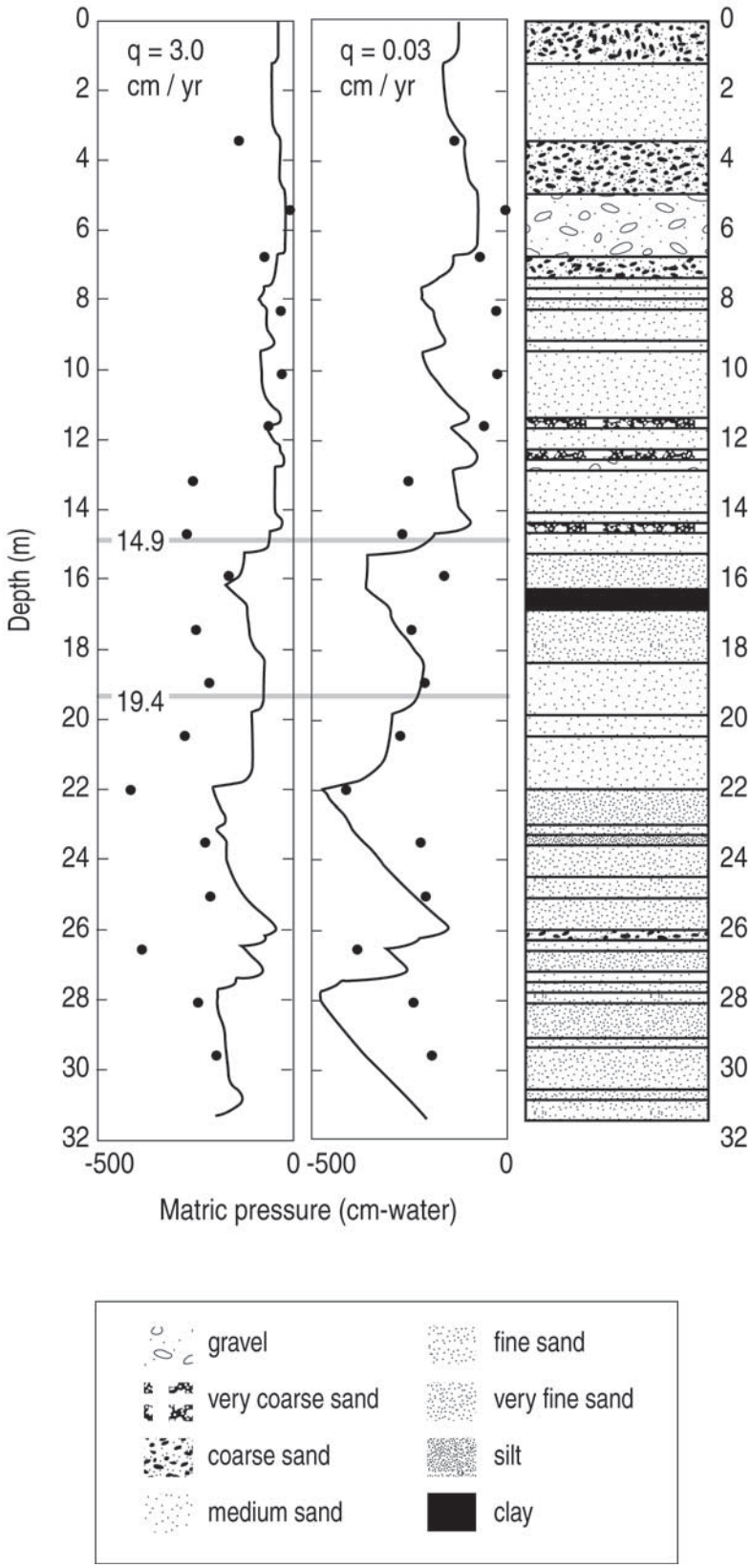

Figure 6. Simulated matric pressure profiles for two q values in the lower Oro Grande Wash. Points measured at the Desert Research Institute [*Izbicki et al.*, 2000a] shortly after core retrieval are shown as solid dots. The depths of 14.9 and 19.4 m are explicitly labeled to indicate the positions of the samples for which K was measured. Soil lithologies, as estimated by our procedure (see Appendix A), are also shown as a function of depth.

Table 2. Effect of Flux Density on the Confidence Index, for hole L

Flux density q, cm/s	C_{2X}, %
1E-10	85.43
1E-9	88.00
1E-8	91.99
1E-7	93.21
1E-6	95.22
1E-5	96.69
1E-4[a]	95.27[a]

[a] Perching developed during the numerical simulation.

Table 4. Effect on the Confidence Index of the Exponent l in the K-Scaling Relation (6) for Hole L Assuming a Flux Density of 10^{-7} cm/s

K Exponent l	C_{2X}, %
−1	91.18
−1.5	92.84
−2	93.21
−2.5	95.37
−3	97.67

defined a confidence statistic, C_{2X}, as the probability that the modeled ψ gradient in any given core-sized (4-cm) interval is smaller in magnitude than the gravitational gradient. For the criterion of how great a matric pressure gradient can be tolerated, this statistic has built into it our judgment that an approximate factor-of-2 error from this effect would be the maximum tolerable. We computed C_{2X} for a given modeled profile by dividing it into 4-cm intervals and computing the proportion of these that have matric pressure gradient of lesser magnitude than gravitational force. Thus the numerical value of C_{2X} represents the probability that the error in the flux estimate from assuming a negligible matric pressure gradient is about a factor of two or less.

[36] The values of C_{2X} for the two simulated profiles in Figure 6 are 93% and 88%. Thus the simulations indicate that in either of these cases one can assume with about 90% confidence that the samples came from a depth interval without a substantial ψ gradient. Here "substantial" is taken to mean great enough to cause a factor-of-two deviation of the total driving force from the constant force of earth gravity.

[37] The chief utility of this numerical simulation is in evaluating the sensitivity of the flux estimates to assumptions made in property-estimation and modeling (but not the assumptions related to steadiness and one-dimensionality, discussed elsewhere in this paper). For example the two-order-of-magnitude difference in q noted above (Figure 6) has only a modest effect on the value of C_{2X}. Other factors of particular concern are the scaling of grain sizes, the determination of $K(\psi)$, and the coarseness of the resolution of layer thicknesses. We evaluated the sensitivity of the model to errors from these sources by means of the computed effect on C_{2X} as shown in Tables 2–6. The value of q for these tests was taken to be 10^{-7} cm/s (3 cm/yr). For grain size scaling, we did model calculations with a range of scaling by a factor b, giving different mean grain sizes λ_{bi} according to

$$\lambda_{bi} = b\lambda_i \tag{5}$$

where λ_i is the mean grain size that comes from the procedure outlined in the Appendix. We found that a range of b values from 0.6 to 2.6, applied to the lower hole (as in Figure 6) produced C_{2X} values between 93% and 95%, indicating little sensitivity to the uncertainty of grain sizes (Table 3). Similarly we tested the sensitivity to the accuracy of the inferred $K(\psi)$ by repeating the model calculations with a range of variations in the scaling relations

$$K \propto \lambda^l \tag{6}$$

and

$$\psi \propto \lambda^m \tag{7}$$

where l and m are arbitrarily adjustable parameters. For Miller-Miller scaling, l equals 2 and m equals −1. As Tables 4 and 5 show, the sensitivity of C_{2X} to these parameters is not great. We found somewhat greater sensitivity of C_{2X} to layer thickness (Table 6); changing the average thickness from 0.75 m to 0.075 m, applied in a Monte Carlo-generated configuration of layers, produced C_{2X} values from 96% to 80%. In reality there are thinner layers than our observation and sampling techniques can identify, but the C_{2X} value remained fairly high even in the case of 0.075 m average thickness. For all physically reasonable realizations, the value of C_{2X} stayed high. On the basis of this sensitivity analysis, the point water flux estimates in Figure 5 are acceptable with a fairly high degree of confidence.

Table 3. Effect on the Confidence Index of the Grain Size Multiplier (b in Equation 5) for Hole L Assuming a Flux Density of 10^{-7} cm/s

Grain Size Multiplier b	C_{2X}, %
10	96.64
2.56	94.86
1.6	93.98
1.0	93.21
1/1.6	92.51
1/2.56	91.97
0.1	88.07

Table 5. Effect on the Confidence Index of the Exponent m in the ψ-Scaling Relation (7), for Hole L Assuming a Flux Density of 10^{-7} cm/s

ψ Exponent m	C_{2X}, %
0.5	99.85
0.75	97.14
1	93.21
1.25	90.72
1.5[a]	90.08[a]

[a] Perching developed during the numerical simulation.

Table 6. Effect on the Confidence Index of Layer Thickness, as Generated in Monte Carlo Simulations of Hypothetical Layered Profiles Assuming a Flux Density of 10^{-7} cm/s

Mean Layer Thickness, m	C_{2X}, %
0.75	95.59
0.075	79.75
0.0075	36.01

[38] Reconsidering the recharging flux results in Figure 5 in light of the C_{2X} sensitivity analysis, it is more likely that the significant decline in q with depth results more from unsaturated-zone lateral flow away from the wash than from the nonuniformity of ψ with depth. In borehole L at 15–20 m a substantial impeding layer might cause an increase in lateral flow and consequently a substantial reduction in downward flux density. The finest-textured layer of all, described in the log as a sandy clay, is at 16.1 (±0.3) m depth. The modeled ψ increases sharply just above this layer, and the measured ψ values increase somewhat further above it. This suggests that θ also is higher just above this layer, possibly resulting from a tendency for water accumulation here. Additional support for this hypothesis comes from a comparison of modeled results to the ψ data measured on core samples, at two different q values. Both parts of Figure 6 show the simulations with the measured points for comparison. The simulation with 3 cm/yr fits generally better in upper layers and the simulation with 0.03 cm/yr fits generally better in lower layers. The lesser flux density at greater depths is consistent with a lateral spreading of flow as it goes through layers.

4.5. Two-Dimensional Numerical Simulations

[39] Our two-dimensional steady-state model provides information on the extent of the wetted portion of the unsaturated zone under a streambed, which is likely to be the main zone of interest for the total areal recharge. The model uses the same layer properties as the one-dimensional model, with the layers taken to be infinitely wide and perfectly horizontal. For each model run our chosen initial flux was spread over the width of the streambed, chosen as 2 m [*Lines*, 1995], and the steady-state unsaturated flow equation was solved for downward flux densities at all points in the domain.

[40] Figure 7 shows contour plots of relative downward flux predicted from the two-dimensional model applied to the cross section perpendicular to the channel at L. The spatial pattern of flux is as expected, with spreading beneath and away from the wash. Most of the spreading is at layer boundaries. The most pronounced spreading in the lower hole profile occurs near 16 m depth, at the upper boundary of the finest-textured layer, consistent with the interpretation of the one-dimensional model results. Figures 7a and 7b illustrate the effect of different average particle sizes of the finest layer. Numerical simulations for boreholes M and U exhibit similar behavior, though neither of them has a layer as fine or as influential on spreading as the one at borehole L.

5. Discussion

[41] The determination of unsaturated water fluxes from hydraulic property measurements in a layered profile requires knowledge of the flow properties of the whole profile. High-quality measurement of these properties is essential because poor approximations might lead to fluxes known only to an order of magnitude or worse, which would have little hydrologic value. In practical terms,

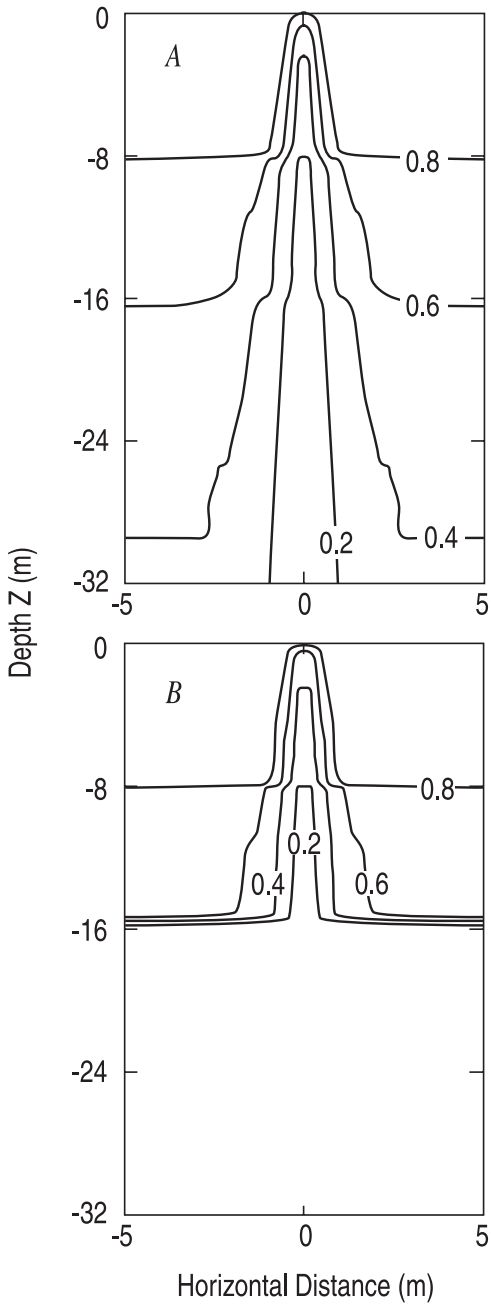

Figure 7. Contour plots of relative downward flux from two-dimensional steady state simulations in the lower Oro Grande Wash. Each contour encloses a specified fraction of the total input flux. For example, 40% of the flux will be within the area bounded above by the 0.4 contour; the narrower this region at any given depth, the more spatially concentrated the flux under the streambed at that depth. These two plots simulated with different hydraulic properties of one of the layers, at 16 m depth. This layer was based on the geometric mean grain size of 0.06 mm in Figure 7a and on the median grain size of 0.00003 mm in Figure 7b.

Table A1. Modified ASTM Soil Classification Scheme Used in Lithology Log Analyses

Classification	Particle Size Range	Geometric Mean
Large pebble sized gravel	37.75–75 mm	53.2 mm
Medium pebble sized gravel	19–37.75 mm	26.8 mm
Small pebble sized gravel	8.99–19 mm	13.1 mm
Granule sized gravel	4.75–8.99 mm	6.18 mm
Very coarse sand	3.08–4.75 mm	3.62 mm
Coarse sand	2.00–3.08 mm	2.48 mm
Medium sand	425 μm–2.00 mm	922 μm
Fine sand	150–425 μm	252μm
Very fine sand	75–150 μm	106 μm
Silt	2–75 μm	12.2 μm
Clay	<2 μm	0.447 μm

however, it is impossible to measure a set of unsaturated hydraulic property data in adequate detail for the large number of samples that would be needed to characterize a complex, heterogeneous profile. Thus the available measured data need to be extended by the generation of surrogate data.

[42] The assumptions we used in generating surrogate data necessarily entail a high degree of approximation. The use of the lower-quality surrogate data, however, is only for verification of the general character of the flow regime. The more accurate SSC-measured hydraulic property data quantify the flux density at specific points. Our sensitivity tests show that the final results of interest are not very sensitive to any particular assumption used in generating surrogate data.

[43] Processes other than those modeled may be significant. For example, tilted layers would put the path of greatest downward flow away from the center of the streambed, thus away from the location where the samples were taken. Contrasting materials in lenses of finite width could have similar effects. Transport of vapor out of the profile could also account for the flux density increase with depth, but this would require significant temperature or solute gradients to drive the vapor flow, and such gradients are unlikely to exist below a few meters' depth [*Izbicki et al.*, 2000b]. It is also possible that the system is not in fact at steady-state, that a change in the hydrology, possibly human-induced, has altered the flow rate below the streambed and the system has not yet had time to reequilibrate [*Izbicki et al.*, 2000b]. Given that poorly understood processes may be significant, our approach is to formulate a consistent quantitative picture of the unsaturated-zone flow without these processes, with awareness that they can be incorporated into this picture as more information becomes available.

[44] Besides the validity of the essential assumptions, the accuracy of interpreted flux values depends on the accuracy of the measurements. For the SSC Darcian method applied at two sites, *Nimmo et al.* [1994] estimated uncertainties of about ±20% for flux estimations for most cases, with a ±90% uncertainty for a case where K was highly sensitive to θ in the θ range surrounding the field water content. This type of sensitivity is apparent in many of the $K(\theta)$ curves in Figure 4, suggesting that for this study the uncertainty in flux estimates, exclusive of uncertainty related to horizontal flow and other minimally explored hydrologic issues, falls in the range of ±20% to ±90%. This range can be taken to represent a base uncertainty, to which would be added the uncertainty from weakness of assumptions.

[45] The values of our measured fluxes give some confirmation of other estimates of unsaturated water fluxes below depths of about 15 m at this site. The trend is consistent, for measurements at comparable depths in the three widely separated boreholes. The data do not suggest a substantial variation in recharge rate with distance downstream, though the sparsity of measured points is probably inadequate for a conclusive answer on this issue. Flux densities at depths of 19 to 30 m for the three holes range from 2 to 6 cm/yr, in good agreement with results of tracer studies, which, given an average water content of 0.1, indicate q of about 7 cm/yr down to 30 m depth [*Izbicki et al.*, 1998]. The horizontal water fluxes generated by these layers are likely also to be hydrologically significant, for example as related to horizontal solute transport [e.g., *Striegl et al.*, 1996]. The results are also relevant to the total areal recharge of a stream such as the Oro Grande Wash. If spreading behavior can be quantified sufficiently through measurements at various depths, a model that approximates experimental results can indicate the total flux passing through the streambed, which would be the input flux that produces model results closest to the measurements. For example, two-dimensional inverse modeling could find the input flux that optimizes computed with respect to measured $\psi(z)$. Another way would be to multiply the measured point flux density by the effective area determined by two-dimensional modeled output as in Figure 7.

6. Conclusions

[46] A combined measuring and modeling approach can produce a basic quantitative conceptualization of two-dimensional unsaturated flow through a layered alluvial profile. A few high-quality point measurements of unsaturated K constitute primary data that need to be supplemented with qualitative knowledge of the materials and a Darcian simulation of unsaturated flow through the entire profile. With too few point measurements to directly represent a multilayer heterogeneous system, we approximated the unsaturated hydraulic properties of the unsaturated zone to 32-m depth using scaling assumptions and estimation of scale factors from lithologic descriptions. At a typical location (L) the model has 42 discrete layers. Using these profile property models, we numerically solved Darcy's law in one and two dimensions to obtain values of matric pressure and water flux as a function of position. The key feature of this approach is that the quantitative final results

Table A2. Weighting Factors Used to Interpret Lithology Logs

Constituent	Weight/Factor
Main constituent	4
"–y" modifier, e.g., silty [sand]	2
"with" modifier, e.g., [sand] with silt	1
the word "slightly"	0.5
the word "minor"	0.5
the word "occasional"	0.25
the word "trace"	0.25

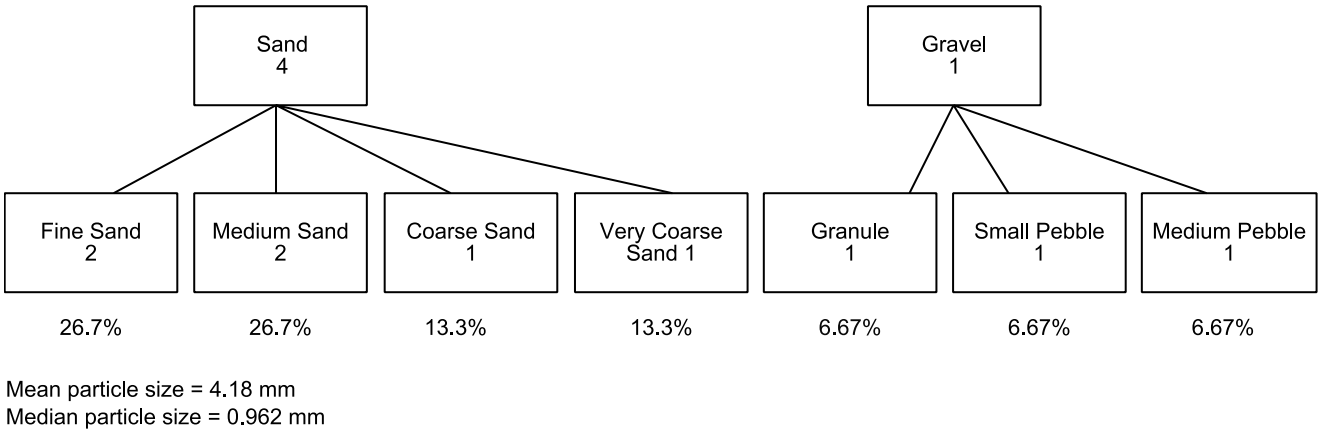

Figure A1. Diagram of weighting procedure for estimating mean particle size of a soil layer. This example is based on the lithology log for the 14.3 to 14.6 m interval of borehole L.

are strongly sensitive to the few high-quality K(Θ) measurements but weakly sensitive to the less accurately known data. We evaluated the sensitivity of the results to various influences, showing the approximating assumptions to have little or negligible effect. The results were most sensitive to layer thickness, though a factor of 10 decrease in average thickness caused only a decline in confidence from 96 to 80%. A single minimally conductive layer can by itself account for a high degree of spreading and decrease of flux density consistent with observations.

[47] Our resulting flux estimates are consistent with those of other methods, such as tracer studies and streamgaging, suggesting flux densities of about 4 cm/yr at depths of several m below the streambed. The character and spatial trends of these estimates also are consistent with a pronounced lateral spreading of flux, especially where it encounters particularly fine-textured layers. Associated with this lateral spreading is a decrease in vertical flux density with depth, spanning about 3 orders of magnitude over the 15-to-50-m interval studied.

[48] Further research could profitably explore the two-dimensional patterns of water flow in a plane perpendicular to the channel, and, with samples from additional boreholes, the variation in fluxes along the channel. The present results show that a few accurate measurements of unsaturated hydraulic conductivity relations combined with a large amount of easily obtained information on the subsurface media permit assessment of water fluxes relevant to subsurface redistribution and aquifer recharge. The confidence associated with the five point measurements and the minimal sensitivity to the approximating assumptions suggest that this approach can reliably quantify unsaturated zone fluxes through strongly layered deposits such as those of the Mojave desert.

Appendix A: Estimation of Particle Sizes from Lithology Logs

[49] To translate each layer's log entry into an approximate particle size distribution, we used the ASTM soil classification scheme [*American Society for Testing and Materials*, 1984]. For our purposes, we modified these classifications. First it was necessary to differentiate between silt and clay on the basis of particle size. The ASTM classifications do this on the basis of plasticity and liquid limits, which are not known for our materials. We adopted the USDA [*Soil Survey Staff*, 1975] clay classification of 2 microns or less; silts ranged from 2 to 75 microns. Second, the driller's log implied further subdivisions, including "very coarse" and "very fine" sands. Therefore, we divided the regions of fine sand and coarse sand into very fine, very coarse to medium fine, and medium coarse. We made these divisions in proportion to those of the USDA system. Considering the area occupied by both fine and very fine sands in the USDA chart, the ratio is 3:2 on a log scale; in the case of coarse and very coarse, the ratio is 1:1 on a log scale. We also divided the ASTM fine gravel category into gravel granules and small pebbles using a logarithmic 1:1 ratio and divided the coarse gravel category into medium and large pebbles in the same fashion. Applying these ratios and our clay/silt distinction, the final scheme is given in Table A1.

[50] For each layer's verbal textural description, we applied a weighting scheme to the various components to determine the mean particle size for each layer. We followed the percentages implied under the ASTM standards for verbal descriptions of soils. This system is described in Table A2. The weightings were normalized to percentages. Each major constituent (sand, silt, gravel, clay) was normalized first within itself, and then the major constituents themselves were normalized. A weighted average was then taken of the geometric means of the particle sizes to arrive at the estimated mean grain size for the layer in question. We conducted linear interpolation between the endpoints of whichever size range contained the median in order to find the median particle size.

[51] As an example, consider layer 18 (14.3 to 14.6 m) of the lower borehole (Figure A1). The log entry is "Slightly gravelly sand, fine to medium sand with some coarse to very coarse sand and granule to medium pebble-sized gravel. . ." Sand, the main constituent, gets a weight of 4. Gravel gets a weight of 2 (gravelly) times a factor of 0.5 (slightly) for a weight of 1. Within the sand category, fine to medium sand is the main constituent, and they each receive a weight of 2 for a total of 4. Coarse sand is assumed to refer to the medium coarse section of the sand range since a

differentiation is made between coarse and very coarse sand in this layer. (Fine sand, by contrast, refers to the entire range of the ASTM fine sand category in this layer, since very fine sand is not discussed.) Therefore, medium coarse and very coarse sands each get a weight of 1 because of the ''with'' modifier. In terms of the gravel, no main constituent is identified so it is assumed to be spread equally among granule, small pebble, and medium pebble sizes, and each gets an equal weight. The total weights of sand and gravel are then normalized to the required overall ratio: all the sand components must combine for a weight of 4 and all gravel components for a weight of 1, as discussed above. The mean particle size is then computed using a weighted average of geometric mean particle sizes in each category. The median particle size is calculated by interpolating within the medium sand category, which contains the median.

[52] **Acknowledgments.** We are indebted to S. Jane Liaw for making the SSC measurements of hydraulic conductivity, to Richard Healy for adapting the VS2DT code for two-dimensional steady-state calculations, and to Scott Tyler and William Albright of the Desert Research Institute for their matric-pressure and particle-size measurements.

References

American Society for Testing and Materials, Standard method for particle-size analysis of soils, in *D422-63, Annual Book of ASTM Standards 04.08*, pp. 116–126, Gaithersburg, Md., 1984.

Campbell, G. S., and G. W. Gee, Water potential: miscellaneous methods, in *Methods of Soil Analysis*, part I, edited by A. Klute, pp. 619–634, Soil Sci. Soc. of Am., Madison, Wis., 1986.

Childs, E. C., *An Introduction to the Physical Basis of Soil Water Phenomena*, John Wiley, New York, 1969.

Deason, J. A., Modeling of groundwater recharge under ephemeral washes in the Mojave River Basin, B.S. honors thesis, Stanford Univ., Stanford, Calif., 1997.

Driscoll, F. G., *Groundwater and Wells*, 1089 pp., Johnson Filtration Syst., Saint Paul, Minn., 1986.

Fayer, M. J., M. L. Rockhold, and M. D. Campbell, Hydrologic modeling of protective barriers; Comparison of field data and simulation results, *Soil Sci. Soc. Am. J.*, *56*, 690–700, 1992.

Gardner, W. R., Some steady-state solutions of the unsaturated moisture flow equation with application to evaporation from a water table, *Soil Sci.*, *85*, 228–232, 1958.

Gardner, W. R., Water movement below the root zone, paper presented at 8th International Congress on Soil Science, Int. Soc. of Soil Sci., Bucharest, Romania, 1964.

Gee, G. W., M. D. Campbell, and J. H. Campbell, Rapid measurement of low soil water potentials using a water activity meter, *Soil Sci. Soc. Am. J.*, *56*, 1068–1070, 1992.

Hammermeister, D. P., D. O. Blout, and J. C. McDaniel, Drilling and coring methods that minimize the disturbance of cuttings, core, and rock formations in the unsaturated zone, Yucca Mountain, Nevada, *Proceedings of the NWWA Conference on Characterization and Monitoring of the Vadose (Unsaturated) Zone*, pp. 507–541, Natl. Well Water Assoc., Worthington, Ohio, 1986.

Healy, R. W., Simulation of solute transport in variably saturated porous media with supplemental information on modifications to the U.S. Geological Survey's computer program VS2D, *U.S. Geol. Surv. Water Resour. Invest. Rep., 90-4025*, 1990.

Izbicki, J. A., R. L. Michel, and P. Martin, Chloride and tritium concentrations in a thick unsaturated zone underlying an intermittent stream in the Mojave Desert, southern California, USA, in *Gambling With Groundwater, Proceedings of IAH and AIH*, edited by J. Brahana, et al., pp. 81–88, U.S. Geol. Surv., Sacramento, Calif., 1998.

Izbicki, J. A., D. A. Clark, M. I. Pimentel, M. Land, J. Radyk, and R. L. Michel, Data from a thick unsaturated zone underlying Oro Grande and Sheep Creek Washes in the western part of the Mojave Desert, near Victorville, San Bernardino County, California, *U.S. Geol. Surv. Open File Rep., 00-262*, 2000a.

Izbicki, J. A., J. Radyk, and R. L. Michel, Water movement through a thick unsaturated zone underlying an intermittent stream in the western Mojave Desert, southern California, USA, *J. Hydrol.*, *238*, 194–217, 2000b.

Klute, A., and C. Dirksen, Hydraulic conductivity and diffusivity, laboratory methods American Society Agronomy, in *Methods of Soil Analysis, Part I*, edited by A. Klute, pp. 687–732, Soil Sci. Soc. of Am., Madison, Wis., 1986.

Lappala, E. G., R. W. Healy, and E. P. Weeks, Documentation of the program VS2D to solve equations of fluid flow in variably saturated porous media, *U.S. Geol. Surv. Water Resour. Invest. Rep., 83-4099*, 1987.

Li, W., B. Li, Y. Shi, D. Jacques, and J. Feyen, Effect of spatial variation of textural layers on regional field water balance, *Water Resour. Res.*, *37*, 1209–1219, 2001.

Lines, G. C., Ground-water and surface-water relations along the Mojave River, southern California, *U.S. Geol. Surv. Water Resour. Invest. Rep., 95-4189*, 1995.

Meisling, K. B., and R. J. Weldon, Late Cenozoic tectonics of the northwestern San Bernardino Mountains, Southern California, *Geol. Soc. Am. Bull.*, *101*, 106–128, 1989.

Mendez, G. O., and A. H. Christensen, Regional water table (1996) and water-level changes in the Mojave River, the Morongo, and the Fort Irwin ground-water basins, San Bernardino County, California, *U.S. Geol. Surv. Water Resour. Invest. Rep., 97-4160*, 1997.

Miller, E. E., Similitude and scaling of soil-water phenomena, in *Applications of Soil Physics*, edited by D. Hillel, pp. 300–318, Academic, San Diego, Calif., 1980.

Miller, E. E., and R. D. Miller, Physical theory for capillary flow phenomena, *J. Appl. Phys.*, *27*, 324–332, 1956.

Nimmo, J. R., and K. C. Akstin, Hydraulic conductivity of a saturated soil at low water content after compaction by various methods, *Soil Sci. Soc. Am. J.*, *52*, 303–310, 1988.

Nimmo, J. R., and K. A. Mello, Centrifugal techniques for measuring saturated hydraulic conductivity, *Water Resour. Res.*, *27*, 1263–1269, 1991.

Nimmo, J. R., J. Rubin, and D. P. Hammermeister, Unsaturated flow in a centrifugal field: Measurement of hydraulic conductivity and testing of Darcy's law, *Water Resour. Res.*, *23*, 124–134, 1987.

Nimmo, J. R., K. C. Akstin, and K. A. Mello, Improved apparatus for measuring hydraulic conductivity at low water content, *Soil Sci. Soc. Am. J.*, *56*, 1758–1761, 1992.

Nimmo, J. R., D. A. Stonestrom, and K. C. Akstin, The feasibility of recharge rate determinations using the steady-state centrifuge method, *Soil Sci. Soc. Am. J.*, *58*, 49–56, 1994.

Nimmo, J. R., A. M. Lewis, and K. A. Winfield, Discernable large-and small-scale features affecting recharge in Abo Arroyo and similar basins, in *U.S. Geological Survey Middle Rio Grande Basin Study-Proceedings of the Fourth Annual Workshop, Albuquerque, New Mexico, February 15–16, 2000*, edited by J. C. Cole, *U.S. Geol. Surv. Open File Rep., 00-488*, 41–43, 2000.

Press, W. H., B. P. Flannery, S. A. Teukolsky, and W. T. Vetterling, *Numerical Recipes*, Cambridge Univ. Press, New York, 1989.

Simmers, I., *Estimation of Natural Groundwater Recharge, Proceedings NATO Advanced Workshop*, D. Reidel, Norwell, Mass., 1988.

Soil Survey Staff, *Soil Taxonomy: A Basic System of Soil Classification for Making and Interpreting Soil Surveys, USDA-SCS Agric. Handbk. 436*, U.S. Gov. Print. Off., Washington, D. C., 1975.

Stamos, C. L., and S. K. Predmore, Data and water-table map of the Mojave River ground-water basin San Bernardino County, California, November 1992, *U.S. Geol. Surv. Water Resour. Invest. Rep., 95-4148*, 1995.

Striegl, R. G., D. E. Prudic, J. S. Duval, R. W. Healy, E. R. Landa, D. W. Pollock, D. C. Thorstenson, and E. P. Weeks, Factors affecting tritium and 14-Carbon distributions in the unsaturated zone near the low-level radioactive-waste burial site south of Beatty, Nevada, April 1994 and July 1995, *U.S. Geol. Surv. Open File Rep., 96–110*, 1996.

J. A. Deason, LECG, LLC, 100 Hamilton Ave., Suite 200, Palo Alto, CA 94301, USA.

J. A. Izbicki and P. Martin, U.S. Geological Survey, 5735 Kearny Villa Rd., Suite O, San Diego, CA 92123, USA.

J. R. Nimmo, U.S. Geological Survey, MS-421, 345 Middlefield Road, Menlo Park, CA 94025, USA. (jrnimmo@usgs.gov)